Spiral Wave Meander in Excitable Media: The Large Core Limit

Vincent Hakim[1] and Alain Karma[2]
[1]*Laboratoire de Physique Statistique, Ecole Normale Supérieure, 24 rue Lhomond, 75231 Paris Cedex 05, France*
[2]*Department of Physics and Center for Interdisciplinary Research on Complex Systems, Northeastern University, Boston, Massachusetts 02115*
(Received 28 March 1997)

We show that the dynamics of spiral waves in excitable media can be reduced to a nonlinear equation of motion for the wave tip that is asymptotically exact in a parameter range where the motion takes place around a large central core region. The onset of meander is shown to occur naturally in this range in the usual free-boundary limit where the medium exhibits an abrupt response to a stimulus. This equation provides a simple understanding of the physical origin of the meandering instability of spiral waves and of the quasiperiodic motion of the wave tip. [S0031-9007(97)03624-7]

PACS numbers: 47.54.+r, 47.20.Hw, 82.40.Bj, 87.22.As

Spiral waves are ubiquitous structures found in a wide range of excitable media and play a crucial role in cardiac arrhythmia [1]. The oldest and best studied instability of these waves is meander [2–8], a term coined by Winfree [2] to distinguish the anomalous motion of the spiral tip in the Belousov-Zhabotinsky reaction from steady-state rotation at fixed period $T_0 \equiv 2\pi/\omega_1$ around a circular core of radius R_0. Theory and experiment now agree qualitatively on several aspects of this instability. First, meander originates from a supercritical Hopf bifurcation [4–7] that introduces a second frequency ω_2 (i.e., the imaginary part of the unstable eigenvalue at onset), which is generally incommensurate with ω_1. Second, the flowerlike meander patterns traced by the wave tip take on universal character near the codimension-2 point where $\omega_2 = \omega_1$ [6,7]. Namely, they exhibit either outward or inward petals depending on whether $\omega_2 - \omega_1$ is positive or negative. Inward and outward petals also correspond to transitions from steady rotation around large and small central core regions, respectively [8,9]. However, what has remained largely missing is an understanding of the physical origin of meander, as opposed to its bifurcation structure. There is presently no simple picture of the destabilizing mechanism giving rise to this instability. In addition, it is not analytically known what determines its onset as a function of the basic parameters of an excitable medium, and what controls physically the frequency ratio ω_2/ω_1 that dictates the meander pattern.

In this Letter, we derive an equation of motion for the spiral wave tip that is asymptotically exact away from the codimension-2 point, in the limit where rotation takes place around a large core region. In this limit, the entire wave tip region can be treated as an essentially rigid body whose slow motion is controlled by local spatial gradients of excitability in the medium. This allows us to rigorously reduce the dynamics of the entire spiral wave to that of a single point. We find that the onset of meander occurs at increasingly larger R_0 and that $\omega_2/\omega_1 \to 1/2$ as the parameter ϵ that controls the abruptness of the response is decreased. We obtain from this analysis a simple picture of the destabilizing mechanism of meander.

We consider the singly ($\gamma = 0$) and weakly diffusive ($\gamma \ll 1$) limits of the standard two-variable reaction-diffusion models of excitable media

$$\partial_t u = \epsilon \nabla^2 u + f(u, v)/\epsilon\,, \tag{1}$$

$$\partial_t v = \gamma \epsilon \nabla^2 v + g(u, v)\,, \tag{2}$$

with a linearly stable rest state (u_0, v_0). These equations reduce for small ϵ to a free-boundary problem [10]:

$$c_n = c(v) - \epsilon\kappa\,, \tag{3}$$

$$\partial_t v = \gamma \epsilon \nabla^2 v + g\big(u^{\pm}(v), v\big)\,, \text{ in } \mathcal{D}^{\pm}, \tag{4}$$

where c_n is the normal velocity of the interface separating the excited and recovery regions of the medium denoted by $(\mathcal{D}^+)$ and $(\mathcal{D}^-)$, respectively, κ is the local curvature of this interface, and $u^{\pm}(v)$ denotes the right-most $(+)$ and left-most $(-)$ branches of the u nullcline $[f(u, v) = 0]$ assumed to have a standard S-shaped function in the (u, v) plane. We measure the excitability of the medium, i.e., the threshold stimulus necessary to cause a response, by the parameter $\Delta \equiv v_s - v_0$, where v_s is the stall value of v at which $c(v_s) = 0$. The isolated pulse speed $c_0 \equiv c(v_0)$ is then a monotonously increasing function of Δ with $c_0 = \alpha\Delta$ for $\Delta \ll 1$.

For a fixed ϵ, R_0 increases monotonously as Δ is decreased and diverges at the *rotor boundary* $\Delta_m(\epsilon)$ with $\Delta_m \sim \epsilon^{1/3}$ for $\epsilon \ll 1$ [11]. This boundary marks the lower excitability limit of spiral wave propagation in the (ϵ, Δ) plane. Exactly on this boundary, the spiral becomes a steady shape translating at c_0 [11] referred to hereafter as the *critical finger*. For $\Delta < \Delta_m(\epsilon)$, the wave tip retracts [8,12]. We shall find that the meandering instability boundary $\Delta_c(\epsilon)$ occurs close to $\Delta_m(\epsilon)$ for small ϵ in agreement with Winfree's exhaustive numerical surveys of the FitzHugh-Nagumo and Oregonator models [8]. Our analysis follows three main steps. We first characterize the spiral tip motion by its tangential velocity c_t and by

 © 1997 The American Physical Society

the radius of curvature R_i of its trajectory (Fig. 1). We then show that on the time scale of interest R_i is a function of c_t that we obtain explicitly. Finally, we determine c_t as a function of the local characteristics of the medium that depend predominantly on the previous passage of the tip at the same angular position in the large core limit.

We define the wave tip as the point of zero normal velocity ($c_n = 0$) on the interface between excited and recovery regions and parametrize it by polar coordinates r_t and θ (Fig. 1). The first purely kinematical part of our analysis, which is independent of Eqs. (3) and (4), consists of deriving an equation of motion for the tip as a point in two-dimensional Euclidean space whose *instantaneous* tangential velocity, c_t, and radius of curvature of trajectory, R_i, are given functions of time. For this purpose, we start from the exact kinematic relations $R_i = c_t^3/\mathrm{Im}[\dot{z}^*\ddot{z}]$ and $c_t = |\dot{z}|$, where $z \equiv r_t e^{i\theta}$, and only assume that R_i and c_t deviate slightly from their steady-state values so that $\delta R_i \equiv R_i - R_0$ and $\delta c_t = c_t - c_t^0$ are small. Using the scalings $\delta R_i \sim q$ and $q/R_0 \sim \delta c_t/c_0$, we obtain at lowest order in q/R_0

$$\ddot{q} + \omega_1^2 q = \omega_1^2 \delta R_i\,, \tag{5}$$

$$\dot{\psi} = 0\,. \tag{6}$$

Equation (6) shows that, in this limit, the nontrivial dynamics comes from the radial motion.

The following part of our analysis consists of deriving an expression for the right-hand side of Eq. (5) directly from Eqs. (3) and (4), which requires us to relate δR_i to the history of the previous passages of the wave tip, i.e., to $q(t')$ for $t' \le t$. Several simplifications make this possible in the large core limit that are summarized here and will be presented in more detail elsewhere [13]. For c_t^0 close to c_0, an analysis of steady rotating spirals shows that they can be decomposed into three regions: (i) a tip region well approximated at lowest order by the critical finger with a tip radius of curvature $R_{\mathrm{tip}} \equiv \epsilon/c_0$, (ii) an outer region where one can neglect curvature effects on the interface velocity in Eq. (4) and where the spiral shape is asymptotically the involute of a circle, and (iii) an intermediate region on distances of order $\sim(R_{\mathrm{tip}}^2 R_0)^{1/3}$ from the spiral tip where the interface is almost normal to the tip circle of rotation and its curvature is small. In this region, the spiral shape is described at dominant order by a integrable Riccati equation.

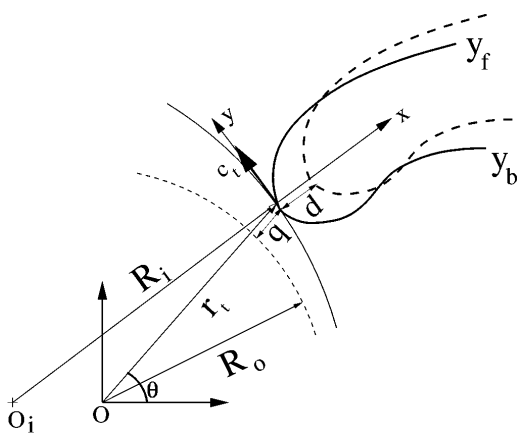

FIG. 1. Coordinates of the wave tip. O and O_i denote the steady state and instantaneous centers of rotation of the tip, respectively. Other variables are defined in the text. The dashed line represents the spiral tip at its previous passage.

Matching these three regions relates R_0 and the tip velocity c_t^0 for steady-state rotation as

$$R_0/R_{\mathrm{tip}} = \mathcal{R}(c_t^0/c_0) \simeq [b/(1 - c_t^0/c_0)]^{3/2}, \tag{7}$$

with the numerical constant $b = -2^{1/3}a_1 \simeq 2.946$ (a_1 is the first zero of Airy function Ai [14]). The asymptotic behavior of $\mathcal{R}$ for $c_t \to c_0$ given by the second equality of Eq. (7) agrees well with a previous numerical determination [12]. This analysis is important for our present purposes because it can be generalized to a nonsteady situation when c_t remains close to c_0 and both R_i and c_t vary on the time scale of the steady rotation period $T_0 = 2\pi R_0/c_t^0$. In this case, the tip region relaxes to a steady-state shape that is well approximated by the critical finger on a time scale $\sim R_{\mathrm{tip}}/c_t$ that is much shorter than the rotation period. Moreover, since the matching region is small compared to R_0, R_i relaxes to a steady-state value on a time scale that is much shorter than T_0 of the order $\sim(R_{\mathrm{tip}}/R_0)^{1/3}T_0$. The key conclusion is that, on the time scale of the rotation period, R_i is related to c_t by the same function [Eq. (7)] that relates R_0 and c_t^0 during steady-state rotation, i.e., $R_i(t)/R_{\mathrm{tip}} = \mathcal{R}[c_t(t)/c_0]$.

To calculate c_t, we start by rewriting Eq. (1) in terms of the local set of orthogonal coordinates (x, y) defined in Fig. 1 with the origin at the tip and the y axis parallel to c_t. We then obtain the coupled equations

$$\epsilon \frac{d^2 y_j}{dx^2} = c_t\left[1 + \left(\frac{dy_j}{dx}\right)^2\right] - c(v_j)\left[1 + \left(\frac{dy_j}{dx}\right)^2\right]^{3/2} \tag{8}$$

describing the wave front ($j = f$) and wave back ($j = b$) in the tip region where $v_f(x)$ [$v_b(x)$] denotes v on the wave front (wave back). Next, v_f and v_b are obtained by integrating Eq. (4) in each region $\mathcal{D}^{\pm}$. This task is simplified by the fact that the width of the excited region is small compared to R_0, and T_0 is large compared to the recovery time constant, $\tau_R \equiv \partial_u f(\partial_u g \partial_v f - \partial_v g \partial_u f)^{-1}|_{u=u^-(v_s),v=v_s}$, over which the system relaxes exponentially to the rest state. Therefore v_f can be assumed to depend only on the radial displacement of the tip, $d(t) \equiv q(t) - q(t - T_0)$ after one complete rotation (Fig. 1). Furthermore, the solution of Eq. (4) is made analytically tractable by assuming that γ is small enough. For $\gamma \ll 1$, one can neglect diffusion entirely in $\mathcal{D}^+$. One can treat diffusion only along x in $\mathcal{D}^-$ if the diffusion length $\ell \equiv \sqrt{4\epsilon\gamma T_0}$ is much shorter than the scale of the matching region $\sim(R_{\mathrm{tip}}^2 R_0)^{2/3}$. This gives $\gamma \ll (R_{\mathrm{tip}}/R_0)^{1/3}$ which requires at the meander boundary the slightly stronger condition $\gamma \ll \epsilon^{1/9}$. Lastly, y_f

(y_b) are given at dominant order by the critical finger front (back) Y_f (Y_b) [which are solutions of Eq. (8) for $c_t = c_0$ [11]]. Using the above simplifications, we obtain the following expressions:

$$v_f - v_0 = \frac{e^{-T_0/\tau_R}}{c_t \tau_E} \int_0^{+\infty} \frac{dx'}{\sqrt{\pi}\ell}\, e^{-(x-x')^2/\ell^2} \times \Theta(x' + d)[Y_f(x' + d) - Y_b(x' + d)], \tag{9}$$

$$v_b = v_f + [Y_f(x) - Y_b(x)]/(c_t \tau_E), \tag{10}$$

where we have neglected terms corresponding to previous passages of the tip at the same angle which are of higher order in e^{-T_0/τ_R}. $\Theta(x)$ is the standard Heaviside step function, and $\tau_E \equiv 1/g(h^+(v_s), v_s)$ is the time constant that controls the plane pulse duration. The condition that there exist solutions of Eq. (8), with the v profiles defined by Eqs. (9) and (10) and the boundary conditions $y_f(0) = y_b(0) = 0$ and $dy_f/dx \to 0$ ($dy_b/dx \to 0$) for $x \to +\infty$, uniquely determines c_t as a function of the parameters of the medium (ϵ, Δ), and d. To implement the above condition, Eq. (8) is linearized around the critical finger by letting $y_j = Y_j + \delta y_j$ ($j = f, b$). Linearization of the wave front equation gives an equation independent of δy_b and that can be solved for δy_f. On the contrary, the linear equation obtained for δy_b, $\mathcal{L}_b \delta y_b = G_b$ can be solved only if a solvability condition is satisfied, because the adjoint operator $\mathcal{L}_b^\dagger$ has a null eigenvector δy_b^0 which vanishes at $x = 0$ and $x = +\infty$ [15]. Requiring that $\int_0^{+\infty} dx\, G_b \delta y_b^0 = 0$ determines c_t as

$$\frac{c_t}{c_0} = 1 + \frac{B - B_c}{K} + \frac{3B_c e^{-T_0/\tau_R}}{K}[I(\tilde{\ell}) + F(\tilde{d}; \tilde{\ell})], \tag{11}$$

where we have defined the rescaled lengths $\tilde{d} \equiv d/R_{\rm tip}$ and $\tilde{\ell} \equiv \ell/R_{\rm tip}$ and plotted the function $F(\tilde{d}; \tilde{\ell})$ in Fig. 2 for different $\tilde{\ell}$. $B \equiv \epsilon/(\alpha^2 \tau_E \Delta^3)$, $B_c = 0.535$, and $K = 0.630$ are numerical constants, and $B = B_c$ defines the rotor boundary $\Delta_m(\epsilon)$. The function $I(\tilde{\ell})$ depends weakly on $\tilde{\ell}$ and $I(0) = 0.624$. The desired equation of motion for the wave tip is now obtained by expressing R_i as a function of q, substituting Eq. (11) for c_t into the relation $\delta R_i/R_{\rm tip} = d\mathcal{R}/dc_t|_{c_t = c_t^0} \delta c_t$. Making the change of variable $\theta = \omega_1 t$ in Eq. (5), this finally gives

$$\frac{d^2\tilde{q}(\theta)}{d\theta^2} + \tilde{q}(\theta) = mF(\tilde{q}(\theta) - \tilde{q}(\theta - 2\pi); \tilde{\ell}), \tag{12}$$

where $\tilde{q} \equiv q/R_{\rm tip}$ and we have defined the parameter

$$m = \frac{9B_c(Kb)^{3/2}}{2(B_c - B)^{5/2}} \exp\left[-\frac{2\pi R_{\rm tip}}{c_0 \tau_R}\left(\frac{Kb}{B_c - B}\right)^{3/2}\right], \tag{13}$$

which can be written in terms of the experimentally measurable curve $R_0(c_0)$ as $m = -c_0/R_{\rm tip} dR_0/dc_0 e^{-T_0/\tau_{rR}}$.

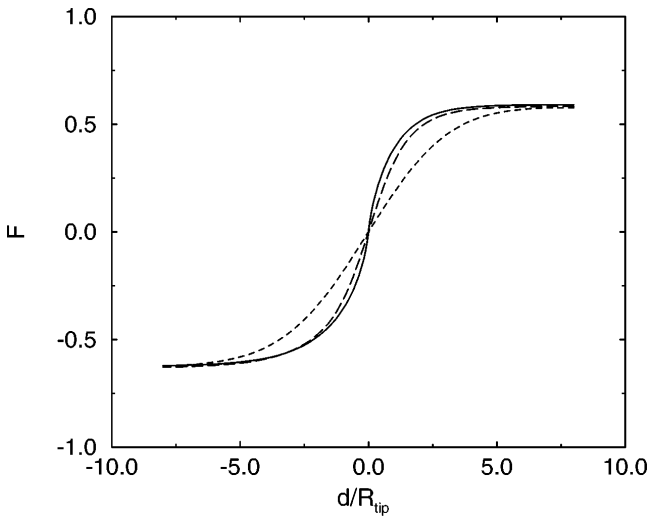

FIG. 2. Plots of $F(\tilde{d}; \tilde{\ell})$ vs $\tilde{d} = d/R_{\rm tip}$ for $\tilde{\ell} = 0$ (solid line), $\tilde{\ell} = 1$ (long-dashed line), and $\tilde{\ell} = 3$ (short-dashed line).

The onset of meander can be determined by examining the stability of Eq. (12) around $\tilde{q} = 0$. Letting $\tilde{q}(\theta) = \hat{q} e^{\Omega\theta}$ and linearizing F, we obtain for $\tilde{\ell} \neq 0$ the eigenvalue equation

$$1 + \Omega^2 = mF'(0; \tilde{\ell})(1 - e^{-2\pi\Omega}), \tag{14}$$

where the two translational modes correspond to $\Omega = \pm i$. This equation admits one complex pair of eigenvalues $\Omega = \Omega_R \pm i\Omega_I$, where Ω_R crosses zero at $m_c = 3/[8F'(0; \tilde{\ell})]$ with $\Omega_I = 1/2$, and $\Omega_R > 0$ for $m > m_c$ (Ω becomes purely real for $m > 3.36 m_c$). This defines the onset of meander and the frequency ratio $\omega_2/\omega_1 = \Omega_I = 1/2$. This prediction is in good quantitative agreement with simulation results presented in Fig. 3 which show that ω_2/ω_1 extrapolates well to $1/2$ at large core radius. Furthermore, a weakly nonlinear analysis of Eq. (12) [13] shows that this Hopf bifurcation is always supercritical with $A_1 \sim \sqrt{m - m_c}$, where $A_1 e^{i\theta/2}$ is the unstable mode. Equation (13) shows that the neutral stability boundary $\Delta_c(\epsilon)$ lies at a distance $\Delta_c - \Delta_m \sim \epsilon^{5/9}/|\ln[\epsilon^{5/9}/F'(0; \tilde{\ell})]|$ away from the rotor boundary in the (ϵ, Δ) plane. This difference becomes vanishingly small in the limit $\epsilon \to 0$, but increases with diffusion at fixed ϵ. This result, if strictly taken, would imply that the onset of meander occurs at Δ_m when $\tilde{\ell} \to 0$ since $F'(0; \tilde{\ell}) \sim -\ln \tilde{\ell}$, in this limit. This can be traced back to the square-root behavior of v_f at $x = -d$ in Eq. (9), which is present only when $\tilde{\ell} = 0$ and gives the small distance behavior $F(\tilde{d}; 0) \sim -\tilde{d} \ln(|\tilde{d}|)$. This nonanalyticity has of course no meaning for lengths d or ℓ smaller than the interface width ϵ and would be cut off in a more refined analysis giving a negligible correction to the meander boundary estimate. This refinement would not alter the tip dynamics on scales $|q| \gg \epsilon$ and is therefore not essential here.

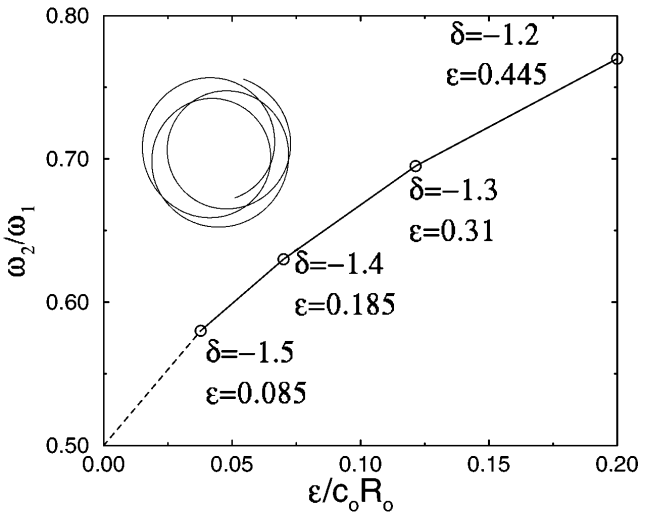

FIG. 3. Plot of ω_2/ω_1 vs $c_0/\epsilon R_0$ obtained by simulations of FitzHugh-Nagumo kinetics with $f(u,v) = 3u - u^3 - v$ and $g(u,v) = u - \delta$ (solid line and circles). $c_0 = (\delta^3 - 3\delta)/2^{1/2}$. The dashed line represents the extrapolation to the asymptotic limit $\omega_2/\omega_1 = 1/2$ predicted by our analysis. These simulations were carried out using a second order accurate direction implicit scheme with $dx/\epsilon = 0.33$ and $dt/\epsilon = 0.1$. The inset shows an example of a large core meander pattern for $\epsilon = 0.180$ and $\delta = -1.4$, where $\omega_2/\omega_1 \simeq 0.67$.

Let us now turn to the physical interpretation of meander contained in Eq. (12). Consider displacing the wave tip by a small distance d towards the outside of its circular trajectory. The right-hand side of Eq. (12) implies that this displacement causes the spiral to rotate on a new radius $R_i = R_0 + \delta R_i > R_0$. This is because the outside of the core is slightly less excitable than the inside, which causes the spiral to rotate on a larger radius. Actually the excitability is reduced by an amount $\sim c_0 e^{-T_0/\tau_R} d/R_{\rm tip}$ due to the previous passage of the spiral at the same angle such that $\delta R_i \sim |dR_0/dc_0|\delta c_0$ for small d. Now, for purely geometrical reasons, if $\delta R_i > d$, the tip will move farther away from the initial circle, causing R_i to increase even further, and thus amplifying the initial displacement. On the contrary, if $\delta R_i < d$, the tip returns closer to this circle, which is stabilizing for the opposite reason. Thus this simple argument predicts that the onset of meanders occurs for $\delta R_i \sim d$, or m of order unity in agreement with the above stability analysis. A similar argument can also be constructed for displacements inside the core. In a nonlinear regime, the amplitude of meander saturates because the excitability gradient only varies on the scale of the tip and F saturates at large $|\vec{d}|$ (Fig. 2). Moreover, the limiting value $\omega_2/\omega_1 \to 1/2$ is due to the fact that θ is completely slaved to t in the large R_0 limit, as implied by Eqs. (6) and (12). Consequently, the previous passage of the tip at the same θ occurs exactly one period T_0 in the past. As R_0 decreases, the first correction to Eq. (6) leads to the modification $\dot{\psi} = -\omega_1 q/R_0$. This correction implies that it actually takes a time T, longer than T_0, for the wave tip to return to the same θ, for outward displacements. This reduces the interaction with the previous tip by an amount $\sim(T - T_0)e^{-T_0/\tau_R}$, and causes the spiral to return sooner inside the core. This leads ω_2/ω_1 to move away from $1/2$ towards unity. A more detailed estimation [13] shows that the order of magnitude of this effect agrees with the numerical results reported in Fig. 3. This points out that the description extends, at least semiquantitatively, to spirals with smaller cores.

In conclusion, we have derived an equation of motion for the spiral wave tip *directly* from the reaction diffusion equations. This has allowed us to obtain a simple physical picture of meander in the large core limit and to understand how its onset depends on the basic parameters of the excitable medium. Several other dynamical aspects of spiral and scroll waves can now be investigated on the basis of this equation [13].

We are grateful to B. Pier for discussions and for performing some computations at an early stage of this work. A. K. thanks Université Paris VII and the Ecole Normale Supérieure for inviting him to Paris and the Laboratoire de Physique Statistique for its hospitality. The research of A. K. is supported by the American Heart Association.

[1] A. T. Winfree, *When Time Breaks Down* (Princeton U. Press, Princeton, NJ, 1987); M. C. Cross and P. C. Hohenberg, Rev. Mod. Phys. **65**, 851 (1993).
[2] A. T. Winfree, Science **181**, 937 (1973); W. Jahnke, W. E. Skaggs, and A. T. Winfree, J. Phys. Chem. **93**, 740 (1989).
[3] T. Plesser *et al.,* J. Phys. Chem. **94**, 7501 (1990).
[4] G. S. Skinner and H. L. Swinney, Physica (Amsterdam) **48D**, 1 (1991).
[5] E. Lugosi, Physica (Amsterdam) **40D**, 331 (1989); A. Karma, Phys. Rev. Lett. **65**, 2824 (1990); D. Barkley *et al.,* Phys. Rev. A **42**, 2489 (1990); Phys. Rev. Lett. **68**, 2090 (1992); I. Mitkov *et al.,* Phys. Rev. E **54**, 6065 (1996).
[6] D. Barkley, Phys. Rev. Lett. **72**, 164 (1994); V. N. Biktashev *et al.,* Int. J. Bifurcation Chaos **6**, 2433 (1996).
[7] G. Li *et al.,* Phys. Rev. Lett. **77**, 2105 (1996).
[8] A. T. Winfree, Chaos **1**, 303 (1991).
[9] A. Belmonte *et al.* (to be published).
[10] J. J. Tyson and J. P. Keener, Physica (Amsterdam) **32D**, 327 (1988); P. C. Fife, J. Stat. Phys. **39**, 687 (1985); P. Pelce and J. Sun, Physica (Amsterdam) **48D**, 353 (1991); A. Karma, Phys. Rev. Lett. **68**, 397 (1992); D. A. Kessler, H. Levine, and W. N. Reynolds, Physica (Amsterdam) **70D**, 115 (1994).
[11] A. Karma, Phys. Rev. Lett. **66**, 2274 (1991).
[12] A. Karma, in *Nonlinear Phenomena Related to Growth and Form,* edited by M. Ben Amar *et al.* (Plenum Press, New York, 1991).
[13] V Hakim and A. Karma (to be published).
[14] M. Abramovicz and I. A. Stegun, *Handbook of Mathematical Functions* (Dover, New York, 1972), p. 478.
[15] For steady states, this was obtained in collaboration with B. Pier [B. Pier, DEA report (ENS, Lyon, 1995)].